Exploration of the Eddy Field in the Midlatitude North Pacific*

WILLIAM J. SCHMITZ, JR.

Woods Hole Oceanographic Institution, Woods Hole, Massachusetts

(Manuscript received 1 July 1987, in final form 28 September 1987)

ABSTRACT

Fourteen moorings were deployed across the midlatitude North Pacific from 165°E to 152°W, for approximately 2 years during 1983–85. Ten mooring sites had previously been occupied at similar latitudes (30°–40°N nominal) for roughly two years (1980–82) along 152°E. Taken together, these observations form the basis for the first systematic basinwide zonal exploration of the eddy field based on moored instrument techniques in the midlatitude North Pacific along the Kuroshio Extension System and North Pacific drift. Eddy kinetic energy (K_E) at abyssal depths decays sharply moving east from 152°E, and has decreased by a factor of 4 by 165°E. There is a plateau in abyssal K_E of about 10 cm^2 s^{-2} across the Emperor Seamounts from 165° to 175°E. Abyssal K_E drops to roughly 5 cm^2 s^{-2} at 175°W and 1 cm^2 s^{-2} at 152°W, for a total decay of a factor of about 50 across the midlatitude North Pacific. Upper level K_E decreases by a total of roughly two orders of magnitude (approximately 10^3 to 10^1) from 152°E to 152°W.

The most energetic sites at 152° and 165°E have essentially the same vertical structure (shape), with the deep and near surface amplitudes at 152°E being 4 and 3 times higher, respectively. In fact, the same type of vertical profile for K_E is appropriate as a first approximation across the entire midlatitude North Pacific, with amplitudes generally decreasing eastward and away from the Kuroshio Extension. Distributions of K_E with frequency are typically peaked somewhat at the mesoscale near the Kuroshio Extension, and generally become more "red" proceeding east and/or toward lower energy areas, although examples of essentially every type of partitioning are available. The K_E values at 165°E are generally the most stable from year-to-year that have ever been measured in energetic regions of the open ocean, at all depths.

1. Introduction

The first long-term moored array across a sizable section of the midlatitude North Pacific (Schmitz et al., 1982) was initially set in 1980 and recovered for the last time in 1982. Observations were made along 152°E from 28° to 41°N across the Kuroshio Extension, in two deployments of ten moorings for roughly a year each. Results from this array and associated XBT and CTD measurements have been presented by Koblinsky et al. (1984), Niiler et al. (1985), Schmitz et al. (1982, 1987), and Schmitz (1984a,b); see also Schmitz and Holland (1986), Bradley (1982), and Levy and Tarbell (1983).

An additional two-year moored instrument data acquisition cycle was initiated in the fall of 1983 to extend this type of data base zonally at midlatitudes. Fourteen moorings were deployed across the North Pacific east of 152°E to 152°W (Fig. 1), with each site occupied for about 2 years. The resulting zonal distribution of abyssal eddy kinetic energy along the Kuroshio Extension has been used for model-data intercomparisons by Schmitz and Holland (1986). Strong and stable abyssal mean currents along 165°E were recently reported by Schmitz (1987). The purpose here is to describe and discuss the zonal distribution of eddy kinetic energy and related properties based on the new observations, along with the 152°E data, including some intercomparison with the North Atlantic. Results based on CTD data acquired on mooring cruises have been published by Joyce (1987), and a moored instrument data report is available (Levy and Tarbell, 1987). Niiler and Hall (1988) and Hu and Niiler (1987) have published results from a moored instrument exploration at 152°W. Talley and White (1988) have summarized some results of a basinwide XBT exploration of the upper layer temperature field in the North Pacific.

2. The data base and methodology

The 14 moorings deployed east of 152°E in Fig. 1, referred to as the zonal exploration array (Table 1), each had current–temperature meters at nominal depths of 150, 650 and 4000 m. The latter are the vertical locations in the absence of currents or errors in

* Contribution Number 6500 from the Woods Hole Oceanographic Institution.

Corresponding author address: Dr. William J. Schmitz, Jr., Woods Hole Oceanographic Institution, Woods Hole, MA 02543.

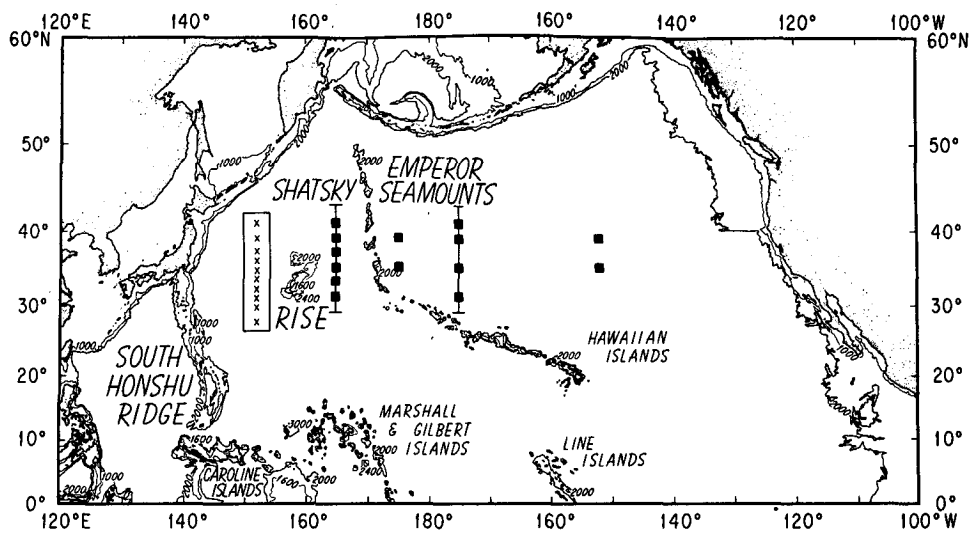

FIG. 1. Mooring locations. Along 152°E, denoted by ×'s enclosed in a rectangular box. The zonal exploration moorings are denoted by solid squares and the thin lines at 165°E and 175°W denote the location of CTD sections. Depth contours (in fathoms) and feature names taken from Chase et al. (1977).

wire and other mooring-component measurement. The first array deployment was from November 1983 to September 1984, with final recovery in October 1985. CTD sections were made on the first two array deployment cruises (Joyce, 1987) at locations indicated on Fig. 1.

Mooring numbers for the first array setting were 793–807 and 815–827 for the second deployment (where one mooring number was aborted due to a problem during launch on each cruise). These mooring numbers are listed and located in Table 1; each latitude and longitude occupied also has a site identifier or number (ZP1 through ZP14, sequentially in order of deployment). Instruments are then identified by adding a digit to the end of the mooring number, starting from the top of the mooring. The first operational moorings that we have ever deployed for an uninterrupted 2-year period, 793 and 794, located at 35° and 39°N along 152°W, were recovered intact and with 100 percent good data. Overall the data return was about 85 percent, with the loss concentrated in one ("new") instrument type (Vector Measuring Current Meter, VMCM), which was deployed on the first setting at 650 m depth along 165°E.

Data were recorded on magnetic tape cassettes. Each record was taken through standard quality control procedures, low-passed as described by Schmitz et al. (1982) and subsampled once per day. The zonal and meridional (x, y) means and variances are denoted by $(\bar{u}, \bar{v})$ and $(\overline{u'^2}, \overline{v'^2})$; the overbar signifies a time average, and a prime superscript indicates the deviation from an average. Eddy kinetic energy (per unit mass, hereafter understood) is $K_E = 0.5(\overline{u'^2} + \overline{v'^2})$. In this context then, "eddies" are not necessarily closed circulation cells or any spatially restricted fluctuation, but encompass the low-frequency variability about the temporal mean. This includes periods longer than two days, and shorter than those covered by the mean (twice the record length by definition).

The discrete Fourier transform procedure employed assigns energy to each of the basic frequency bands (α

TABLE 1. Zonal exploration mooring locations and numbers.

At 165°E	At 175°E	At 175°W	At 152°W
41*N*(801, 821, *ZP*14)		41*N*(795, 827, *ZP*6)	
39*N*(802, 819, *ZP*13)	39*N*(800, 822, *ZP*8)	39*N*(796, 826, *ZP*5)	39*N*(793, *ZP*2)
37*N*(803, 818, *ZP*12)			
35*N*(804, 817, *ZP*11)	35*N*(799, 823, *ZP*7)	35*N*(797, 825, *ZP*4)	35*N*(794, *ZP*1)
33*N*(806, 816, *ZP*10)			
31*N*(807, 815, *ZP*9)		31*N*(798, 824, *ZP*3)	

$\pm 0.5)\tau^{-1}$, where τ is the record length and $\alpha = 1, \cdots, N - 1$; N is one-half the number of data days. The highest frequency ($\alpha = N$) is a cycle per two days and encompasses only half the bandwidth of the lower frequency estimates, as does the mean ($\alpha = 0$), which spans the frequency band from zero to $(2\tau)^{-1}$. The lowest frequency band above the mean contains contributions from the range of periods from ($\frac{2}{3} \rightarrow 2$) τ, "centered" at τ. In calculating frequency distributions, the inverse of the low-pass filter initially used is applied (recoloring) at frequencies lower than 0.5 cycles per day, a matter of consequence primarily for the period range near a few days.

A variety of techniques for describing spectral or frequency distributions may be used, depending on what one wants to emphasize. The summed energy in a few rather broad frequency bands or period ranges in the form of simple bar graphs is the basic time scale description used here; the notation $K_E(a, b)$ designates the eddy kinetic energy in the range of periods from a to b days (or the frequency band b^{-1} to a^{-1} cycles per day). In these bar graphs, the integrated K_E for the band indicated is the ordinate; this presentation is less subject to confusion than attempts to visually estimate area. The period ranges considered here are consistent with those employed, for example, by Schmitz et al. (1982) and Imawaki and Takano (1982). They (nominal) are $K_E(20, 150)$, the temporal mesoscale; $K_E(150, 2\tau)$, τ = record length, secular scale; $K_E(2, 20)$, the "high" frequency band. $K_E(a, b)/\Sigma$, where Σ is the total K_E for all frequency bands considered (plotted), is used when "spectral shape" is being intercompared.

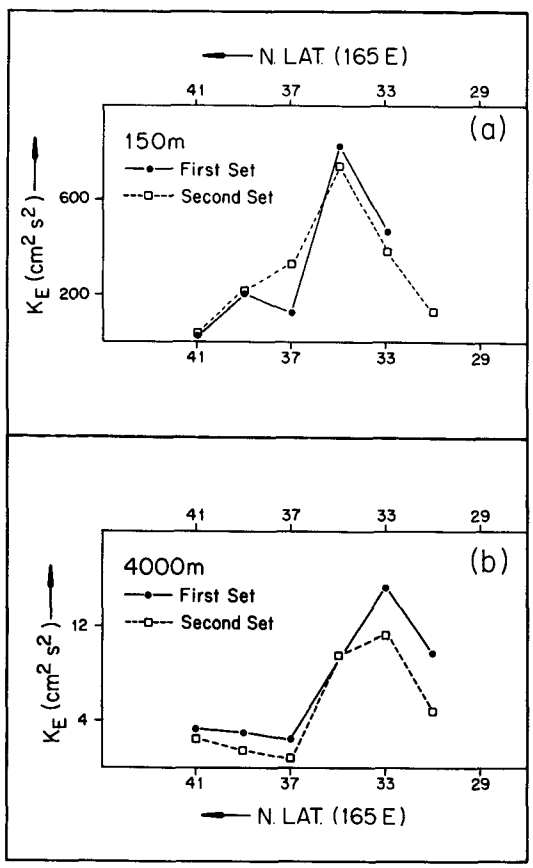

FIG. 2. Eddy kinetic energy K_E along 165°E: (a) at 150 m depth; (b) at 4000 m depth. Solid dots denote the first array setting, open squares the second, each deployment being roughly a year (see text).

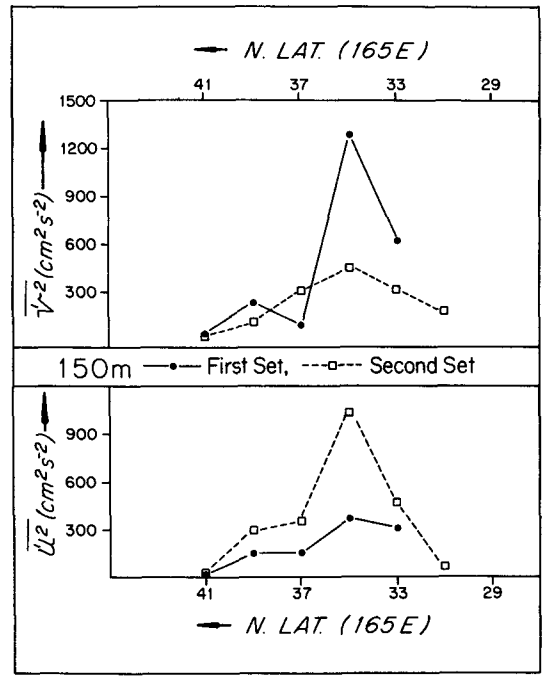

FIG. 3. Zonal ($\overline{u'^2}$) and meridional ($\overline{v'^2}$) variances along 165°E at 150 m depth, for both array deployments. Solid dots denote the first setting, open squares the second.

3. Discussion

Upper level K_E observations along 165°E are strongly reproducible in pattern and even comparatively stable pointwise (Fig. 2a) from year-to-year or deployment-to-deployment, as are the 4000 m or abyssal K_E's (Fig. 2b). This stability in K_E is notable relative to the variability of the associated zonal and meridional variances (Fig. 3). The change in the directionality of the upper level eddy field (also observed at 4000 m) in Fig. 3 is accompanied by a change in the orientation of the associated mean flow (Fig. 4). The most prominent changes in $\overline{u'^2}$ and $\overline{v'^2}$ in Fig. 3 occur at 35°N, the location of the maximum change in mean flow on Fig. 4. The primary variation in Fig. 4 is in the sign of the meridional flow near 35°N, a change in orientation

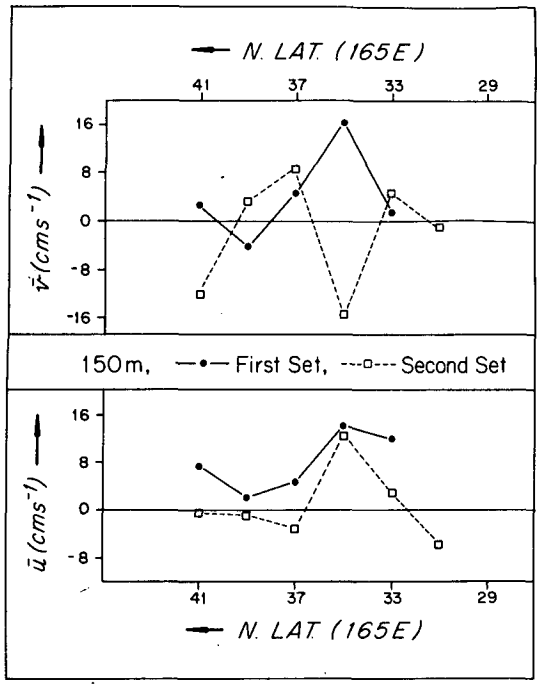

FIG. 4. Mean flow components ($\bar{u}$ zonal, $\bar{v}$ meridional) at 150 m depth along 165°E, for both settings of the moored array. Solid dots denote the first deployment, open squares the second.

of the Kuroshio Extension. For the yearly averages near 35°N in Figs. 3 and 4, when the Kuroshio Extension was oriented northeast, $\overline{v'^2}$ was larger than $\overline{u'^2}$; when the orientation was southeast, the zonal variance dominated. The abyssal K_E's in Fig. 2 are about 1.5–2 times as large as observations by Hamann and Taft (1987) at 167°E, both for latitudes near 35°N. The year-to-year agreement in K_E in Fig. 2 is the best the author has seen anywhere in the open ocean, as is also the case for the mean flows at 165°E (Schmitz, 1987).

The pointwise variability in upper level K_E from deployment to deployment associated with meandering of the Kuroshio Extension previously observed at 152°E (Schmitz et al., 1987) is not prominent in the zonal exploration data, to some extent possibly due to the larger latitudinal sampling interval, especially at 165°E. Distributions of K_E with latitude for 175°W (Fig. 5), analogous to those for 165°E in Fig. 2, are less reproducible in pattern than at 165°E from year to year at the upper levels, and less energetic (Fig. 6) by a factor of 2–5 (for 2-year averages). The maximum values of K_E at 175°W tend to have a somewhat more southerly location than at 165° or 152°E at abyssal depths, and for the first year of observation at all depths.

Figure 7 compares the variation of abyssal K_E as a function of longitude along the axes of the Kuroshio Extension and the Gulf Stream. The peak of the Atlantic distribution is located farther east from the boundary than is the case for the North Pacific. Figures 8 and 9 are maps with abyssal K_E observations superimposed, for the North Pacific and North Atlantic respectively. The abyssal North Pacific is much less energetic than the North Atlantic in the west but they are of comparable intensity in the east (1–5 cm^2 s^{-1}). Note that the maximum abyssal K_E values along 165° and 175°E (Fig. 8) are about the same (13 vs 12 cm^2 s^{-2}) crossing the Emperor Seamounts, toward the southern end of the sections. Measurements that have been made a few to several degrees north and south of the two sites at 35° and 39°N along 152°W (Hu and Niiler, 1987) are close to the results on Figs. 7 and 8. Measurements of abyssal K_E at (30°–31°N, 157°–158°W) by Taft et al. (1981) averaged 1.6 cm^2 s^{-2}, slightly higher than found here (Fig. 8) at 35°N and very close to the value at 28°N observed by Hu and Niiler (1987).

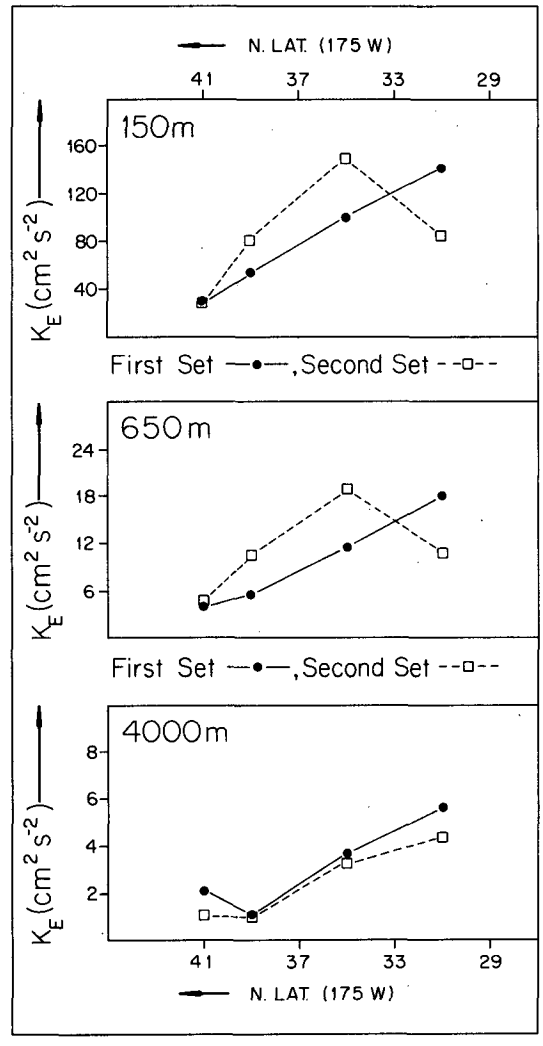

FIG. 5. The K_E along 175°W at three depths. Solid dots denote the first, open squares the second array setting.

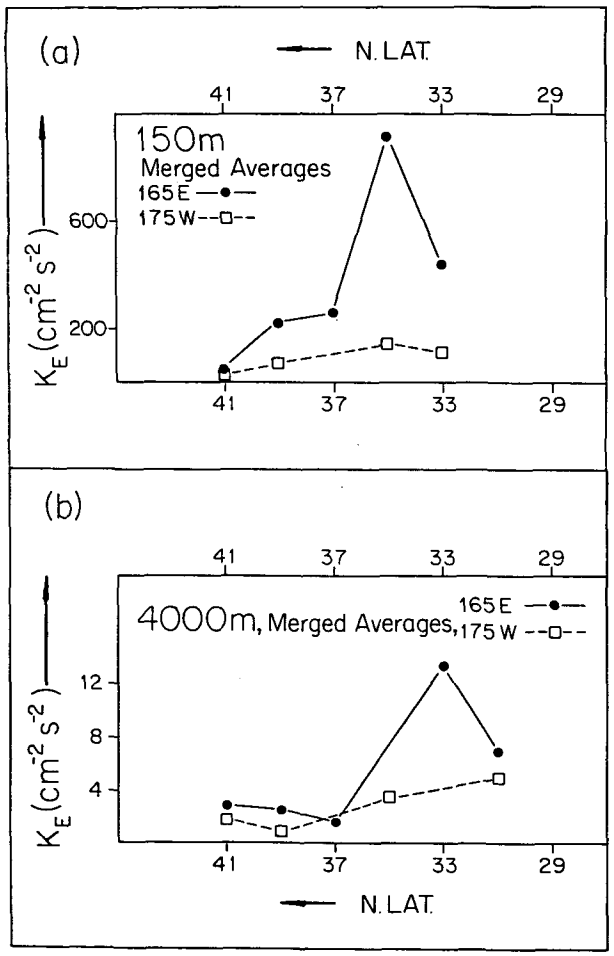

FIG. 6. A comparison of K_E along 165°E and 175°W. Solid dots denote the first array deployment, open squares the second, at two depths: (a) 150 m, (b) 4000 m.

The vertical structure of K_E for the most energetic sites at 152° and 165°E (in the immediate vicinity of the Kuroshio Extension, moorings 724 and 817 at 35°N along 152°E and 165°E, respectively) is compared in Fig. 10a. Differences between moorings 817 and 724 as a function of depth are quantified in Fig. 10b at the same interpolated depths. The functional fits used to interpolate in Fig. 10b are shown in Fig. 11. The standard deviations of the data from the exponential distributions in Fig. 11, which have the same vertical scale, are only 8–9 cm^2 s^{-2}. In Figs. 11a and 11b, the standard deviation is denoted by σ (in cm^2 s^{-2} for K_E), and the symbols and values for the exponential fits are listed on the plots. The "barotropic" or abyssal K_E for the Kuroshio Extension is ~40 cm^2 s^{-2} at 152°E and ~10 cm^2 s^{-2} at 165°E (Fig. 11). The amplitude of the baroclinic component (surface minus abyssal value) is about 3 times larger at 152°E (Figs. 10, 11). Thus the largest K_E at 152°E is 3–4 times more energetic than at 165°E (in the Kuroshio Extension). The stability of the vertical distribution for K_E at these Kuroshio Extension sites at 152° and 165°E is evident in Fig. 12. Looking across the entire data set, upper level K_E (~150–300 m depth) varies from a maximum of about 1000 cm^2 s^{-2} at 152°E to roughly 100 cm^2 s^{-2} at 152°W. These results are in general agreement with the zonal decay scales of the temperature variance map recently presented by Talley and White (1988; their Fig. 3).

Site ZP8 (39°N) is at the location along 175°E where there is two-year data return at all depths. At this site K_E is exceptionally stable at 150 and 4000 m. At the southernmost site along 175°W (Fig. 13), K_E is very stable at the abyssal and 650 m levels but is less so at 150 m depth. Comparing Figs. 13a and 13b demonstrates that either dividing the time series at site ZP3 (31°N, 175°W) into equal pieces or using the somewhat unequal duration mooring deployment records does not lead to any noticeable difference in vertical structure. Comparing Figs. 14 and 11 demonstrates that sites across the North Pacific from 152°E to 152°W have, as a first approximation, similar vertical K_E distributions. At most of these locations K_E distributions

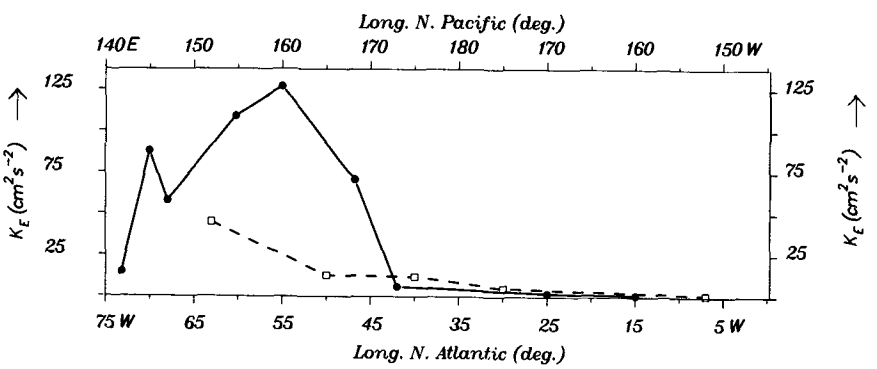

FIG. 7. Abyssal K_E versus longitude for the North Pacific (open squares and dashed line) and North Atlantic (dots and solid line), approximately along the axes of the Kuroshio Extension and Gulf Stream, respectively.

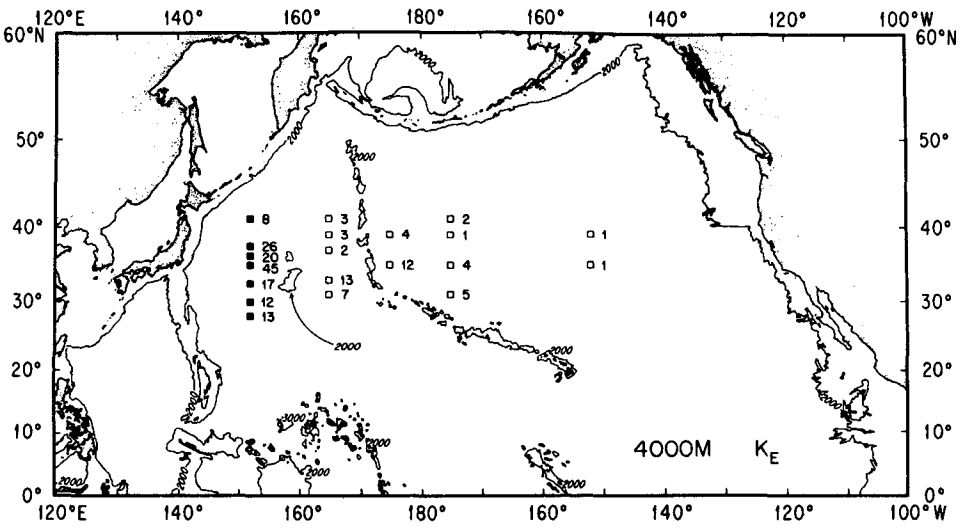

FIG. 8. A map showing abyssal K_E observations for the North Pacific. K_E values in cm^2 s^{-2} are listed next to site locations, denoted by solid squares at 152°E, open squares for the zonal exploration array.

are well approximated by an exponential with 250 m vertical decay scale but differing amplitudes. No special significance should be attached to an exponential distribution; it is simply a specific way to demonstrate similar vertical scale, or to interpolate.

Normalized K_E frequency distributions for 150 m depth at 33°N, 165°E for both deployments there are contained in Fig. 15. These distributions are roughly similar in shape to analogous observations along 152°E (Schmitz, 1984b). Figure 16 contains the normalized frequency distributions for the other vertical levels on mooring 806 (33°N, 165°E). The abyssal frequency

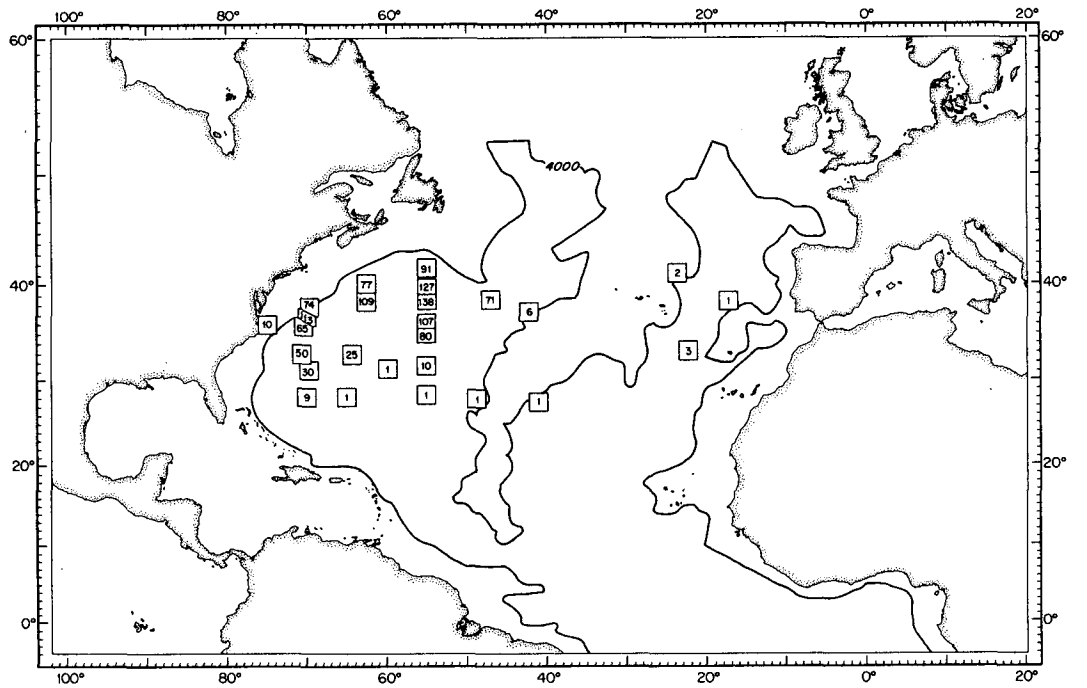

FIG. 9. A map containing selected abyssal K_E observations (cm^2 s^{-2}) from the North Atlantic, modified from Schmitz (1984c).

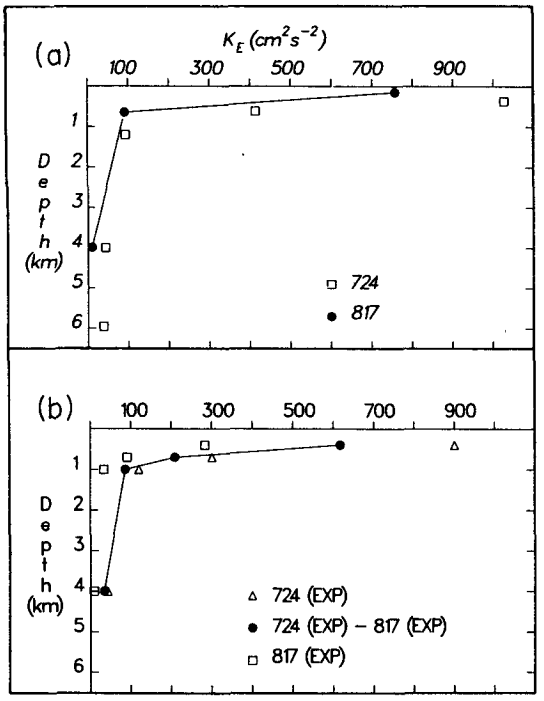

FIG. 10. The vertical distributions of K_E at sites near the Kuroshio Extension (35°N) along 152°E (mooring 724) and 165°E (mooring 817): (a) At the depths that instruments were deployed, (b) Interpolated to standard depths, using exponential (denoted EXP) fits (see Fig. 11).

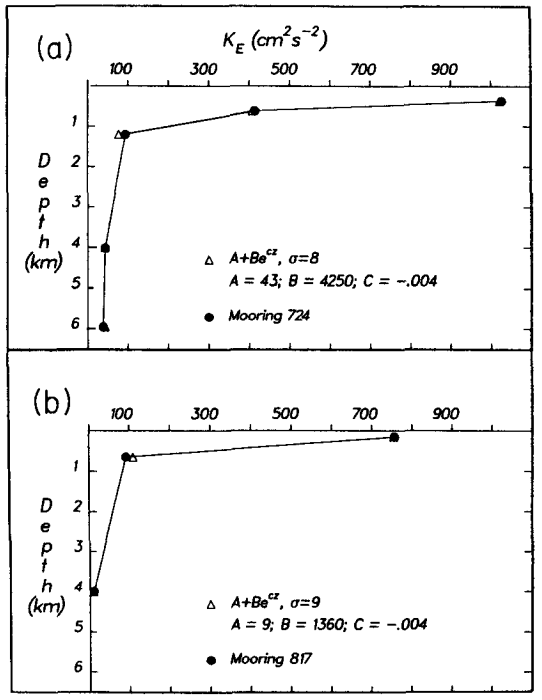

FIG. 11. The functions used to interpolate in Fig. 10: (a) Mooring 724 (35°N, 152°E), and (b) Mooring 817 (35°N, 165°E). The parameters for the exponential fits are listed on the figures (in cm^2 s^{-2} or m^{-1}), along with the standard deviation (σ) of the data from the fit.

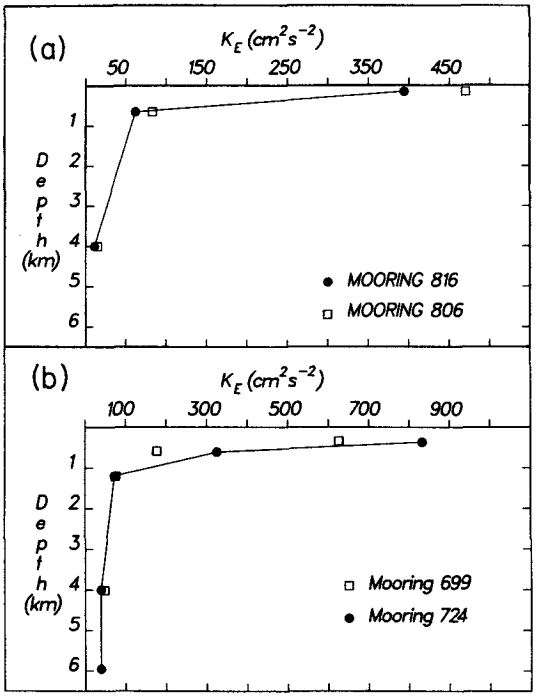

FIG. 12. Variations of the vertical distribution of K_E from deployment to deployment for sites near the Kuroshio Extension: (a) at moorings 806 and 816 at 33°N along 165°E, and (b) at moorings 724 and 699 at 35°N along 152°E. "Two-year" averages are also shown.

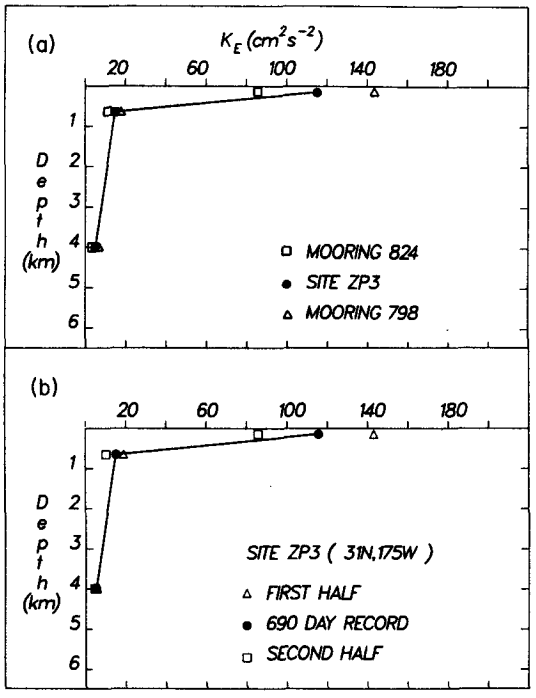

FIG. 13. The vertical distribution of K_E at site ZP3, 31°N and 175°W: (a) for the first and second mooring deployments, (b) for equal half-lengths of the composite time series. "Two-year" averages are also shown.

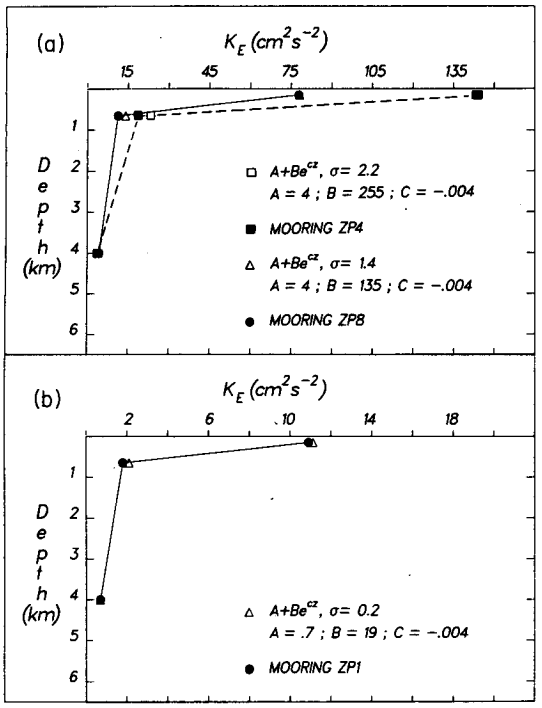

FIG. 14. Exponential fits with the same vertical scale (250 m) for K_E at indicated sites: (a) ZP4 (35°N, 175°W) and ZP8 (39°N, 175°E), (b) ZP1 (35°N, 152°W). The parameters for the exponential fits are listed (in cm^2 s^{-2} or m^{-1}), along with the standard deviation (σ) of the data from the fit.

distribution for both settings (moorings 800 and 822) at the northernmost site (39°N, site ZP8) along 175°E is stable and K_E is a maximum in the highest frequency band (the opposite of "red," Fig. 17) although the 650 m results at mooring 822 show a dramatic increase in K_E in the lowest frequency band. Schmitz et al. (1982) observed similar but less dramatic "high frequency" bottom trapping at 28°N, 152°E. Spectra for sites along 175° and 152°W increase with increasing period as is typically found in lower energy areas in both the North Pacific and the North Atlantic (Fig. 18 is an example).

In the spectral figures (numbers 15 to 18) discussed in the last paragraph, all of which present K_E or normalized K_E as a function of frequency for the same three broad bands, an example of nearly each type of possible distribution is presented. In the vicinity of the Kuroshio Extension or at abyssal depth, the mesoscale (20–150 day periods) band usually has the largest K_E (Figs. 15 and 16). At one particular site (Fig. 17) K_E increases with increasing frequency, becoming a maximum in the 2–20 day range. In low energy areas (Fig. 18), particularly at thermocline depths and above, K_E typically increases with increasing period (frequency distribution is "red").

4. Summary and conclusions

Fourteen moorings were recently deployed from 165°E to 152°W across the midlatitude North Pacific, for approximately 2 years during 1983–85. Ten mooring sites were previously occupied for roughly two years (1980–82) at 152°E. Taken together, these observations form the basis for the first zonal exploration of the eddy field in the midlatitude North Pacific along the Kuroshio Extension System based on moored techniques.

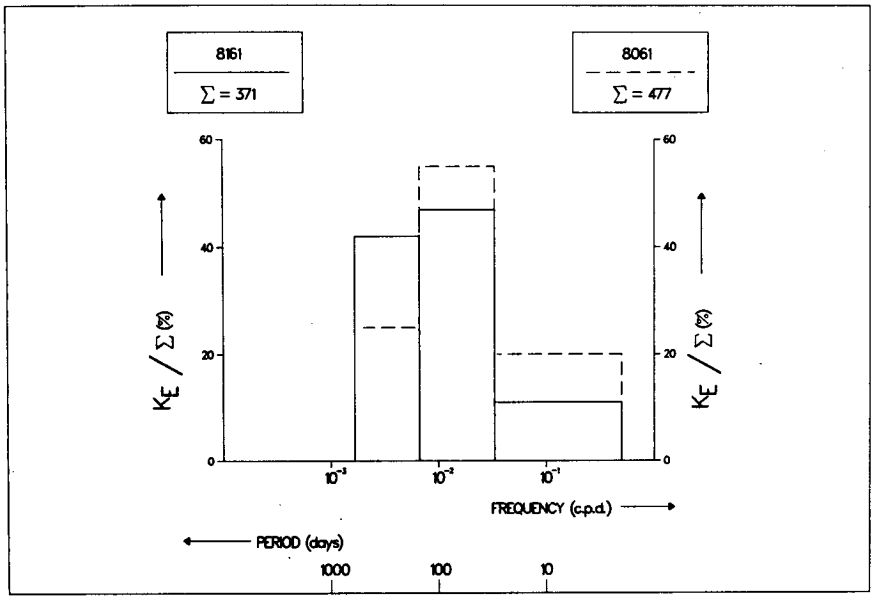

FIG. 15. The normalized frequency distribution of K_E at 8161 and 8061 (33°N, 165°E; Site ZP10). Σ denotes the total K_E in the frequency bands plotted.

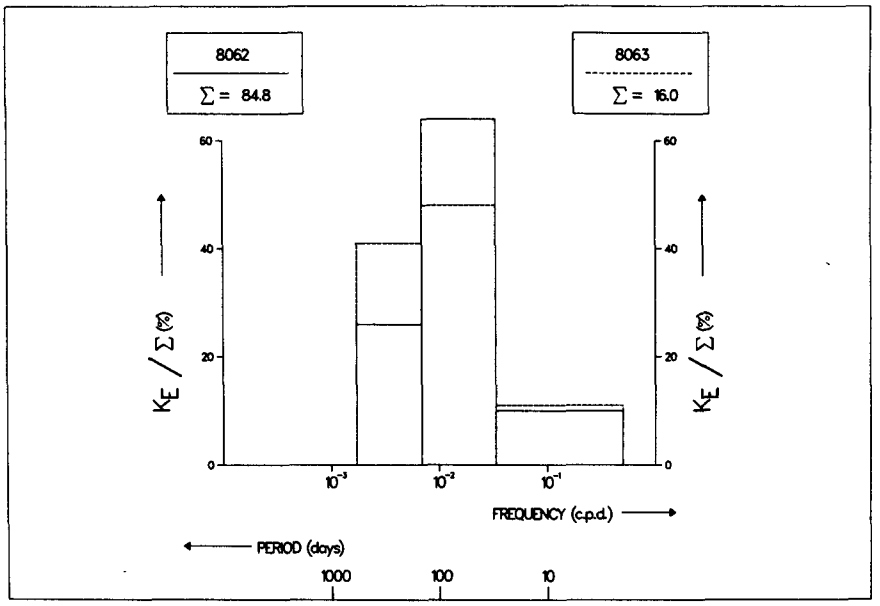

FIG. 16. As in Fig. 15 but for records 8062 and 8063 (33°N, 165°E).

Eddy kinetic energy distributions along 165°E are remarkably stable from year to year. This is especially notable for the upper levels (~150 m) where K_E is reduced from values observed at 152°E by a factor of 2–5. Upper level K_E values decay sharply east from 165°E as well, from about 10^3 to 10 cm^2 s^{-2} across the North Pacific. At abyssal levels, there is no significant change in maximum K_E across the Emperor Seamounts from 165° to 175°E. Beyond 175°E, abyssal K_E decays to roughly 1 cm^2 s^{-2} at 152°W, from approximately 50 at 152°E.

The vertical structure of K_E is also relatively stable, both temporally and zonally. The vertical distribution of K_E for the most energetic sites at 152° and 165°E has the same shape but the deep and near surface amplitudes are 4 and 3 times higher at 152°E. An exponential fit is a good approximation for K_E at midlatitudes along all longitudes across the Pacific, with a ver-

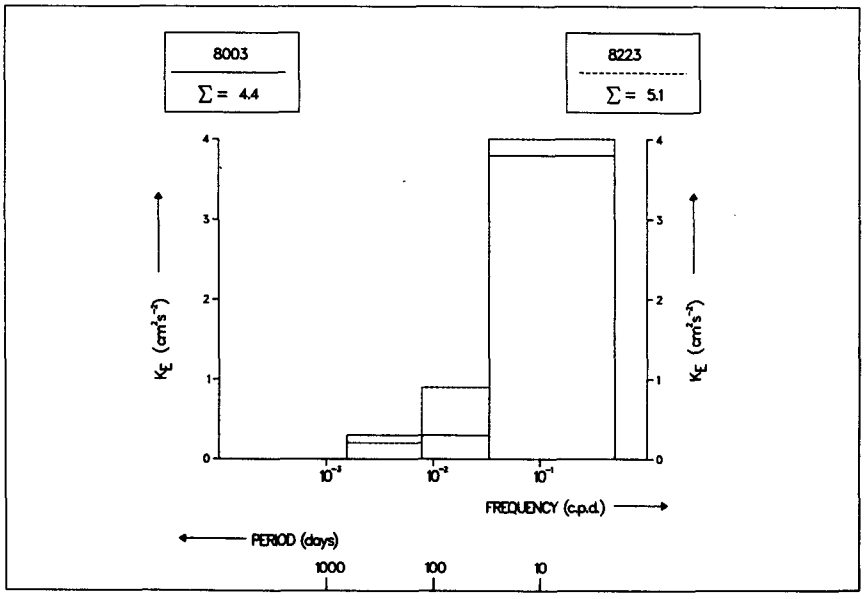

FIG. 17. The frequency distribution of K_E at Moorings 8003 and 8223, both at site ZP8 (39°N, 175°E).

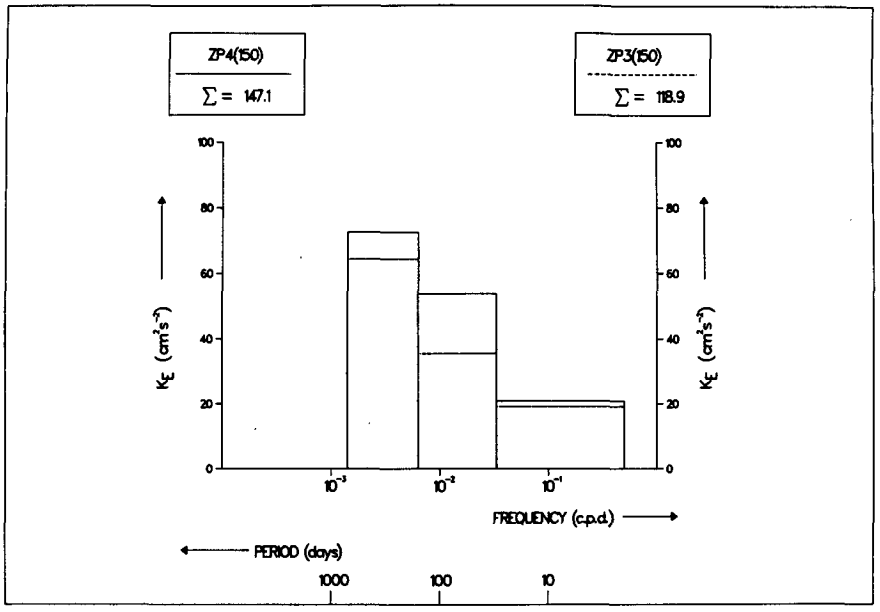

FIG. 18. As in Fig. 17 but at 150 m for sites ZP3 and ZP4 (31° and 35°N, 175°W).

tical decay scale of 250 m. In the higher energy areas, K_E is normally a maximum at the temporal mesoscale (the period range 20–150 days). Frequency distributions change shape, becoming more "red" proceeding east and/or toward lower energy areas, a common result for the North Atlantic as well.

Acknowledgments. This investigation was supported by the Office of Naval Research under Contracts N00014-76-C-0197, NR 083-400 and N00014-84-C-0134, NR 083-400.

REFERENCES

Bradley, K. F., 1982: Technical activities associated with an exploratory array in the western North Pacific. Woods Hole Oceanographic Institution Tech. Rep. WHOI-82-41, 40 pp.

Chase, T. E., H. W. Menard and J. Mammerickx, 1977: Topography of the North Pacific. Tech. Rep. Ser. TR-17, Inst. of Mar. Resources, University of California, La Jolla, 10 pp.

Hamann, I., and B. A. Taft, 1987: The Kuroshio Extension near the Emperor Seamounts. *J. Geophys. Res.*, **92,** 3827–3839.

Hu, J. H., and P. P. Niiler, 1987: NEPAC current meter and XBT data. *S.I.O. Ref. No. 87-4,* 15 pp.

Imawaki, S., and K. Takano, 1982: Low-frequency eddy kinetic energy spectrum in the deep western North Pacific. *Science,* **216,** 1407–1408.

Joyce, T. M., 1987: Hydrographic sections across the Kuroshio Extension at 165°E and 175°W. *Deep-Sea Res.*, **34,** 1331–1352.

Koblinsky, C. J., R. L. Bernstein, W. J. Schmitz, Jr. and P. P. Niiler, 1984: Estimates of the geostrophic stream function in the western North Pacific from XBT surveys. *J. Geophys. Res.*, **89,** 10 451–10 460.

Levy, E., and S. A. Tarbell, 1983: A compilation of moored current meter data from the western Pacific, Vol. XXXI, (1980–1982). Woods Hole Oceanographic Institution Tech. Rep. WHOI-83-30, 60 pp. + 7 microfiche.

——, and ——, 1987: A compilation of moored current meter data from the North Pacific (the "Zonal" Experiment, 1983–1985), Volume XLI. Woods Hole Oceanographic Institution Tech. Rep. WHOI-87-20, 54 p. + 8 microfiche.

Niiler, P. P., and M. M. Hall, 1988: Low frequency eddy variability in the eastern North Pacific subtropical gyre. Submitted to *J. Phys. Oceanogr.*

——, W. J. Schmitz, Jr. and D. K. Lee, 1985: On the geostrophic volume transport in high eddy energy areas of the Kuroshio Extension and Gulf Stream. *J. Phys. Oceanogr.*, **15,** 825–843.

Schmitz, W. J., Jr., 1984a: Abyssal eddy kinetic energy levels in the western North Pacific. *J. Phys. Oceanogr.*, **14,** 198–201.

——, 1984b: Observations of the vertical structure of the eddy field in the Kuroshio Extension. *J. Geophys. Res.*, **89,** 6355–6364.

——, 1984c: Abyssal eddy kinetic energy in the North Atlantic. *J. Mar. Res.*, **42,** 509–536.

——, 1987: Observations of new, large, and stable abyssal currents at midlatitudes along 165°E. *J. Phys. Oceanogr.*, **17,** 1309–1315.

——, and W. R. Holland, 1986: Observed and modeled mesoscale variability near the Gulf Stream and Kuroshio Extension. *J. Geophys. Res.*, **91,** 9624–9638.

——, P. P. Niiler, R. L. Bernstein and W. R. Holland, 1982: Recent long-term moored instrument observations in the western North Pacific. *J. Geophys. Res.*, **87,** 9425–9440.

——, P. P. Niiler and C. J. Koblinsky, 1987: Two-year moored instruments results along 152°E. *J. Geophys. Res.*, **92,** 10 826–10 834.

Taft, B. A., S. R. Ramp, J. G. Dworski and G. Holloway, 1981: Measurements of deep currents on the central North Pacific. *J. Geophys. Res.*, **86,** 1955–1968.

Talley, L. D., and W. B. White, 1988: Estimates of time and space scales in the midlatitude North Pacific from the TRANSPAC XBT survey. *J. Phys. Oceanogr.*, **17,** 2168–2188.